

The Optical Gravitational Lensing Experiment. Variable Baseline Microlensing Events in the Galactic Bulge.*

L. Wyrzykowski^{1,2}, A. Udalski¹, S. Mao³,
 M. Kubiak¹, M.K. Szymański¹, G. Pietrzynski^{1,4},
 I. Soszynski^{1,4} and O. Szewczyk¹

¹ Warsaw University Observatory, Al. Ujazdowskie 4, 00-478 Warszawa, Poland
 e-mail:(wyrzykow,udalski,mk,msz,pietrzyn,soszynsk,szewczyk)@astrouw.edu.pl

² Institute of Astronomy, University of Cambridge, Madingley Road,
 Cambridge CB3 0HA, UK

³ University of Manchester, Jodrell Bank Observatory, Macclesfield,
 Cheshire SK11 9DL, UK
 e-mail: smao@jb.man.ac.uk

⁴ Universidad de Concepción, Departamento de Fisica, Casilla 160-C,
 Concepción, Chile

ABSTRACT

We present the first systematic search for microlensing events with variability in their baselines using data from the third phase of the Optical Gravitational Lensing Experiment (OGLE-III). A total of 137 candidates (88 new) was discovered toward the Galactic bulge. Among these, 21 have periodic oscillations in their baselines, 111 are irregular variables and 5 are potential long period detached eclipsing binaries. This is about 10% of the total number of constant baseline events. They are hence quite common and can be regarded as a new type of exotic events, which allow the determination of extra parameters of the events. We show that microlensing of variable stars may allow us to break the degeneracy between the blending parameter and magnification. We note that in some cases variability hidden in the baseline due to strong blending may be revealed in highly magnified events and resemble other exotic microlensing behavior, including planetary deviation. A new system (VEWS) for detecting ongoing variable baseline microlensing events is presented.

Key words: *gravitational lensing - Galaxy: center - Stars: oscillations - Catalogs*

1 Introduction

In the 1990's the first generation microlensing surveys detected first cases of microlensing events (MACHO – Alcock *et al.* 1993, OGLE – Udalski *et al.* 1993), as predicted by Paczyński (1986), opening the new field of modern astrophysics. Since then several thousand events have been discovered, mostly toward the Galactic bulge and the rate of detection now is around 600 per year in real-time systems (*e.g.*, the Early Warning System – EWS[†], Udalski 2003). One of the main selection criteria applied in events' search algorithms was a requirement of constant baseline light curve before and after the brightening episode. This was used to minimize the risk of a mistake and interpreting a variable star as a microlensing event. Some exploding stars which may mimic

*Based on observations obtained with the 1.3 m Warsaw telescope at the Las Campanas Observatory of the Carnegie Institution of Washington.

[†]<http://ogle.astro.uw.edu.pl/ogle3/ews/ews.html>

microlensing usually exhibit variable baseline. Unfortunately this also excluded variable stars in the sample of stars searched for microlensing. However, variable stars are microlensed with the same probability as other stars and because variability is present in about 10% of the Galactic bulge stars, these events cannot be neglected. If discovered they would add about 60 events to 600 being detected every year, which is a significant number, especially for statistical studies of microlensing in the Galactic bulge, *e.g.*, the determination of the optical depth. So far only a few events with clear variability in the baseline were detected, mostly by accident, *e.g.*, MACHO-SMC-1 (*e.g.*, Udalski *et al.* 1997b) or BUL1.725 (Mizerski and Bejger 2002).

In this paper we present the results of the first systematic search for variable baseline events in the OGLE-III Galactic bulge data covering seasons 2001–2004. We discovered a total of 137 (88 new) candidate events, among which 21 have periodic oscillations in their baselines, 111 are irregular variables and 5 are potential long period detached eclipsing binaries. We present simple models of periodic baseline microlensing events, analyze the behavior of the amplitude of variability during gravitational magnification and show that the change of amplitude of brightness variation during the microlensing allows a direct determination of the blending fraction in some events. This method was recently successfully applied to the event MACHO 97-SMC-1 (Assef *et al.* 2006), which exhibits periodic variability in its baseline. We show that these events are common and can be regarded as a new type of exotic microlensing events, from which additional information (*e.g.*, distance to the source or lens) can be extracted when combined with further spectroscopic observations. We conclude the paper by presenting an extension to the OGLE Early Warning System (EWS), which can detect microlensing episodes of variable stars in real-time and allows frequent followup in order to take full advantage of this type of events.

2 Model of Microlensing Event with Variable Baseline

Whenever the variability in the baseline is regular and predictable in any moment of time it is possible to find a good model of the microlensing event of a variable star. As ground-based microlensing surveys always deal with very crowded fields, observed star-like objects are usually a composite of several individual stars. Variability of at least one of these blended stars will be observed as a change of brightness in the whole composite object. During a microlensing event light of one of the stars is magnified. Thus, there are two classes of such microlensing event models with variable baseline, depending on whether the variable component is magnified or just acts as a blend. For brevity, we refer to the first as a “variable source” event and the second as a “variable blend” event.

If $I_{\text{var}}(t)$ is an analytical or approximated function of the baseline magnitude variability (*e.g.*, from Fourier series fit or interpolation between phase-

folded baseline data points), the addition to the minimum brightness flux due to variability equals to:

$$f_{\text{var}}(t) = 10^{0.4|I_0 - I_{\text{var}}(t)|} - 1 \quad (1)$$

where I_0 is in this case the minimum magnitude of the variable baseline (see Fig. 2 for an illustration). In the case where the variable source is microlensed, the flux relative to the minimum baseline value is given by:

$$f(t) = (f_s + f_{\text{var}}(t))A(t) + f_b. \quad (2)$$

In the case where the variability comes from a blended, unlensed variable star, we have

$$f(t) = f_s A(t) + (f_b + f_{\text{var}}(t)). \quad (3)$$

In Eqs.(2)–(3) f_s denotes the fraction of the total flux contributed by the lensed source to the composite at the minimum brightness of the baseline, and $f_b (\equiv 1 - f_s)$ is the fraction of light contributed by any additional blend.

$A(t)$ is the microlensing magnification, in the simplest case of single point mass lens given in the standard form (Paczynski 1986):

$$A(t) = \frac{u(t)^2 + 2}{u(t)\sqrt{u(t)^2 + 4}}, \quad u(t) = \sqrt{u_0^2 + \tau(t)^2}, \quad \tau(t) = \frac{t - t_0}{t_E} \quad (4)$$

where u_0 is the minimum impact parameter in units of the Einstein radius at the moment t_0 , and t_E is the Einstein radius crossing time.

3 Variability Amplitude in the Microlensing Event

Using the above microlensing model, we can examine the behavior of the variability amplitude during a microlensing event involving a variable star. In the simplest case of a single variable star, its amplitude of variability (ΔI_A) does not change with amplification A and remains equal to the amplitude in the baseline (ΔI_{base}), as the ratio of the amplified to the baseline flux variations is constant.

However, when the lensed variable star is blended with some additional constant flux, the observed amplitude will increase with A as:

$$\Delta I_A = 2.5 \log \left[1 + \frac{\Delta f A}{f_s A + f_b} \right] \quad (5)$$

where $\Delta f = 10^{0.4\Delta I_{\text{base}}} - 1$ is the baseline variability amplitude.

In the theoretical limit of infinite amplification the observed amplitude approaches some constant value, which is the amplitude of the variability of the star we would measure if there were no blending. This real amplitude equals to $2.5 \log \left(1 + \frac{\Delta f}{f_s} \right)$ and its dependence on the blending and baseline variability amplitude is shown in Fig. 1.

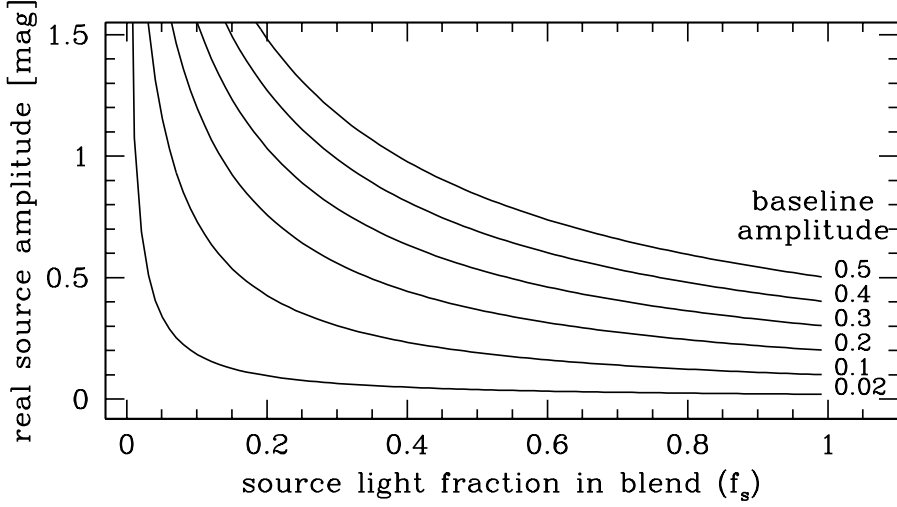


Fig. 1. The dependence of the real amplitude of variability, ΔI_A , on the blending parameter, f_s . The baseline variability amplitude, ΔI_{base} , is indicated for each curve.

This implies that in the case of very strong blending and/or small intrinsic amplitude the variability in the baseline may be buried in the photometry noise and undetectable, making the baseline resembling that of a constant star. However, the hidden variability may then be revealed thanks to microlensing and it will show deviations in the light curve from the standard shape, especially near the peak of magnification. This effect should be considered especially in the case of high magnification events in the crowded Galactic bulge fields, as the variation of brightness due to lensed source variability may be mistaken with other microlensing effects, *e.g.*, finite source size, parallax or planetary deviation.

As the observed amplification (A_{obs}) in a blended event is not the real microlensing amplification, the latter is related to the blending by:

$$A_{\text{unblended}} = \frac{A_{\text{obs}} - 1}{f_s} + 1. \quad (6)$$

A simple calculation of flux changes during microlensing of a variable source star using Eq. (6) leads to:

$$f_s = \Delta f \frac{F_1 - 1}{F_2 - F_1 - \Delta f}, \quad F_1 = 10^{0.4D_{\text{mag}}}, \quad F_2 = 10^{0.4(D_{\text{mag}} + \Delta I_A)} \quad (7)$$

D_{mag} is the magnification in magnitudes, measured along the bottom of microlensed variable light curve from I_0 , and ΔI_A is the amplitude expected at

that magnification. Fig. 2 shows modeled variable baseline light curve with D_{mag} , ΔI_A , I_0 and ΔI_{base} marked. Eq. (7) is a simple formula, which allows one to derive the blending parameter directly from the light curve using its quantities. The accuracy of this formula is limited by the accuracy with which we can measure the variability amplitude during the event. It can be used to complement the usual value obtained from fitting the data with the model of a variable microlensed source (Eq. 2), or in the case of well sampled detached eclipsing binaries even as a substitute. Fig. 3 shows an example diagram for determining the blending parameter for an event with a baseline variability amplitude of 0.2 mag.

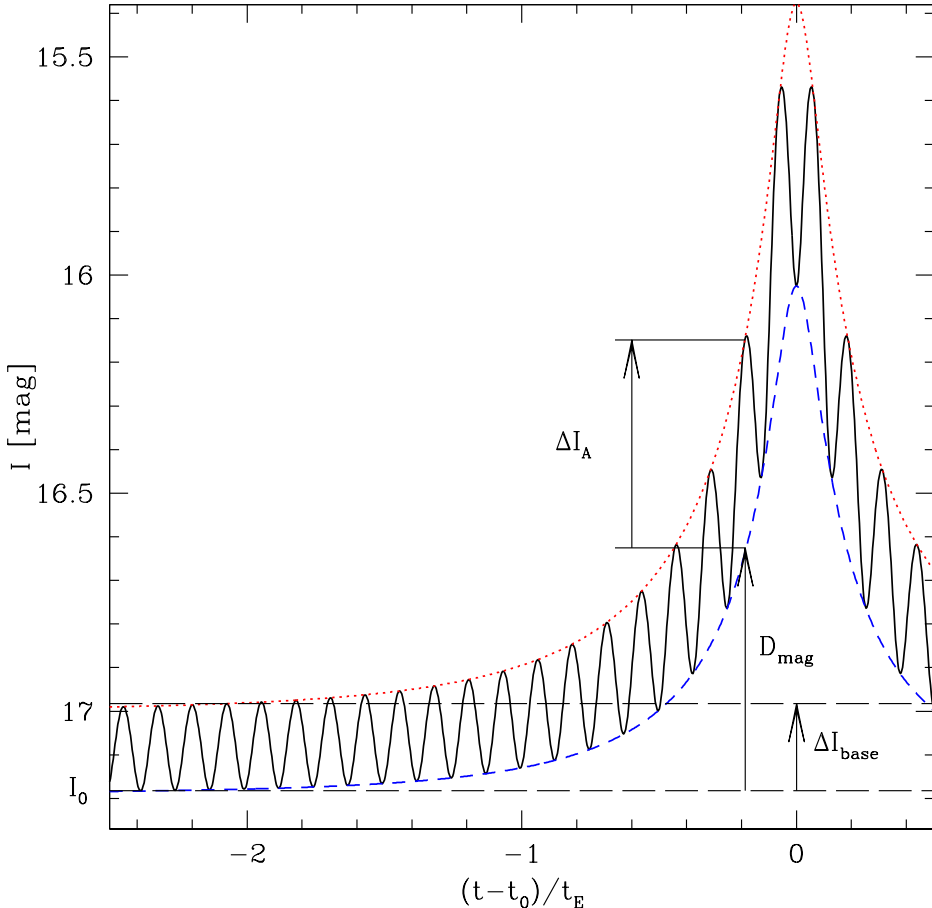


Fig. 2. Synthetic light curve of a variable source microlensing event. The dotted and short-dashed lines outline the amplitude of brightness variability. The bottom long-dashed line represents the minimum baseline magnitude I_0 . D_{mag} , ΔI_{base} and ΔI_A from Eq. (7) are labeled.

When the variability observed in the composite object comes from one of the blending stars and the microlensed star is constant, the observed amplitude will decrease with amplification:

$$\Delta I_A = 2.5 \log \left[1 + \frac{\Delta f}{f_s A + f_b} \right]. \quad (8)$$

With A increasing to infinity the amplitude declines and vanishes completely at the peak.

In the case of a variable blend, because of Eq. (6), it is not possible to obtain a similar relation to Eq. (7) and the only way to measure the blending fraction in such a microlensing event is through fitting the data with a model (Eqs. 3 and 4).

4 Observational Data

All photometric data presented in this paper were collected with the 1.3-m Warsaw Telescope at the Las Campanas Observatory, Chile, which is operated by the Carnegie Institution of Washington, during the third phase of the OGLE project. OGLE-III CCD mosaic camera consists of 8 CCD detectors, 2048×4096 pixels of $15 \mu\text{m}$ size each. Every pixel corresponds to a $0.^{\prime\prime}26$ scale, thus the whole 8192×8192 pixel mosaic gives a field of view of $35' \times 35'$. More details about the telescope and the instrumentation can be found in Udalski, Kubiak and Szymański (1997a) and Udalski (2003).

All images collected by the OGLE-III telescope were de-biased and flat-fielded with the automatic software almost in real-time. Then, they were processed by the photometric data pipeline (Udalski 2003) using the image subtraction method, based on the Woźniak's (2000) implementation of the Difference Image Analysis (DIA) technique (Alard and Lupton 1998). Finally, all photometric measurements for all stars in given field were stored in the OGLE database (*e.g.*, Szymański and Udalski 1993), separately for each filter and chip of the mosaic.

Since its beginning in 2001 OGLE-III observed about 300 fields with different frequency. Among them we selected 82 which were monitored frequently in seasons 2001–2004, *i.e.*, had at least 150 data points in the I -band, in which the vast majority of the observations were taken. The total number of stars brighter than 21 mag (the rough OGLE telescope limit), in all 82 fields is about 100 million, varying from 800 thousand to 2 million per field. Table 1 presents equatorial coordinates of all the selected fields.

It is commonly known that the errors obtained with the DIA photometry are generally under-estimated (*e.g.*, Woźniak 2000), especially for bright stars. Alard and Lupton (1998) attribute photometry scatters larger than the Poisson noise to significant movement of the centroid of the star due to atmospheric effects. Various solutions of this problem for the OGLE-III microlensing events were applied up-to-date, *e.g.*, Snodgrass *et al.* (2004), Collinge (2004), but in

T a b l e 1
Equatorial coordinates (J2000) of centers of the selected 82 OGLE-III fields

field	α_{2000}	δ_{2000}	field	α_{2000}	δ_{2000}
BLG100	17 ^h 51 ^m 00 ^s .43	-30°04'21".6	BLG175	18 ^h 03 ^m 28 ^s .19	-31°19'22".1
BLG101	17 ^h 53 ^m 40 ^s .61	-29°54'25".4	BLG176	18 ^h 06 ^m 09 ^s .29	-31°19'22".3
BLG102	17 ^h 56 ^m 20 ^s .64	-29°35'24".8	BLG179	17 ^h 50 ^m 00 ^s .36	-30°43'50".7
BLG103	17 ^h 56 ^m 20 ^s .60	-30°10'55".6	BLG180	17 ^h 52 ^m 40 ^s .25	-30°43'53".2
BLG104	17 ^h 59 ^m 00 ^s .66	-29°32'50".2	BLG181	17 ^h 55 ^m 20 ^s .11	-30°43'51".3
BLG105	18 ^h 01 ^m 40 ^s .03	-29°32'45".9	BLG182	17 ^h 58 ^m 00 ^s .48	-30°43'50".6
BLG108	17 ^h 46 ^m 29 ^s .73	-36°38'43".0	BLG183	18 ^h 00 ^m 40 ^s .04	-30°43'50".2
BLG115	17 ^h 54 ^m 59 ^s .54	-36°03'19".5	BLG184	18 ^h 03 ^m 18 ^s .41	-30°43'53".3
BLG117	17 ^h 49 ^m 18 ^s .11	-35°27'49".4	BLG185	18 ^h 06 ^m 01 ^s .00	-30°43'53".1
BLG119	17 ^h 54 ^m 56 ^s .17	-35°27'50".6	BLG188	17 ^h 59 ^m 00 ^s .64	-30°08'32".4
BLG121	17 ^h 46 ^m 28 ^s .63	-34°52'16".8	BLG189	18 ^h 01 ^m 39 ^s .48	-30°08'30".4
BLG122	17 ^h 49 ^m 17 ^s .69	-34°52'23".9	BLG190	18 ^h 04 ^m 28 ^s .47	-30°08'30".0
BLG129	17 ^h 43 ^m 43 ^s .64	-34°16'44".8	BLG193	18 ^h 12 ^m 25 ^s .41	-30°08'30".4
BLG130	17 ^h 46 ^m 30 ^s .76	-34°16'45".4	BLG194	17 ^h 51 ^m 00 ^s .21	-29°29'01".2
BLG131	17 ^h 49 ^m 17 ^s .75	-34°16'46".1	BLG195	17 ^h 53 ^m 38 ^s .80	-29°18'53".7
BLG132	17 ^h 52 ^m 04 ^s .73	-34°16'47".5	BLG196	18 ^h 04 ^m 27 ^s .69	-29°32'40".2
BLG133	17 ^h 54 ^m 51 ^s .74	-34°16'47".9	BLG197	18 ^h 07 ^m 04 ^s .75	-29°32'55".4
BLG134	17 ^h 57 ^m 38 ^s .65	-34°16'47".4	BLG198	18 ^h 09 ^m 42 ^s .68	-29°32'55".5
BLG138	17 ^h 45 ^m 15 ^s .24	-33°41'14".3	BLG205	17 ^h 57 ^m 16 ^s .84	-28°57'43".6
BLG139	17 ^h 48 ^m 00 ^s .12	-33°41'16".0	BLG206	17 ^h 59 ^m 53 ^s .28	-28°57'33".3
BLG140	17 ^h 50 ^m 45 ^s .18	-33°41'25".2	BLG208	18 ^h 05 ^m 08 ^s .83	-28°57'33".4
BLG141	17 ^h 53 ^m 30 ^s .27	-33°41'20".4	BLG219	18 ^h 10 ^m 30 ^s .46	-28°22'05".3
BLG142	17 ^h 56 ^m 15 ^s .58	-33°41'36".9	BLG220	18 ^h 13 ^m 06 ^s .43	-28°22'05".5
BLG147	17 ^h 49 ^m 45 ^s .43	-33°06'04".5	BLG225	18 ^h 04 ^m 30 ^s .63	-27°46'31".6
BLG148	17 ^h 52 ^m 36 ^s .75	-33°06'05".8	BLG226	18 ^h 07 ^m 05 ^s .75	-27°46'32".6
BLG149	17 ^h 55 ^m 15 ^s .67	-33°06'06".7	BLG227	18 ^h 09 ^m 39 ^s .95	-27°46'32".3
BLG150	17 ^h 58 ^m 00 ^s .67	-33°06'06".6	BLG232	18 ^h 00 ^m 00 ^s .07	-27°10'59".1
BLG155	17 ^h 52 ^m 18 ^s .04	-32°30'32".3	BLG236	18 ^h 10 ^m 20 ^s .52	-27°11'01".8
BLG156	17 ^h 55 ^m 01 ^s .07	-32°30'33".7	BLG249	18 ^h 06 ^m 00 ^s .55	-25°59'51".6
BLG157	17 ^h 57 ^m 44 ^s .20	-32°30'33".8	BLG250	18 ^h 08 ^m 32 ^s .97	-26°00'00".2
BLG158	18 ^h 00 ^m 27 ^s .14	-32°30'35".8	BLG251	18 ^h 11 ^m 07 ^s .91	-26°00'01".0
BLG160	18 ^h 05 ^m 53 ^s .28	-32°30'34".9	BLG252	18 ^h 13 ^m 39 ^s .54	-25°59'53".7
BLG163	17 ^h 52 ^m 45 ^s .08	-31°54'46".3	BLG333	17 ^h 35 ^m 30 ^s .51	-27°14'34".2
BLG164	17 ^h 55 ^m 27 ^s .07	-31°54'45".9	BLG339	17 ^h 47 ^m 00 ^s .35	-22°34'33".0
BLG165	17 ^h 58 ^m 08 ^s .87	-31°54'46".8	BLG340	17 ^h 49 ^m 30 ^s .56	-22°34'27".4
BLG166	18 ^h 00 ^m 51 ^s .02	-31°54'47".8	BLG342	17 ^h 46 ^m 30 ^s .11	-23°09'56".1
BLG167	18 ^h 03 ^m 32 ^s .99	-31°54'48".5	BLG343	17 ^h 49 ^m 00 ^s .20	-23°09'55".1
BLG171	17 ^h 52 ^m 44 ^s .51	-31°19'20".6	BLG346	17 ^h 42 ^m 00 ^s .67	-24°21'02".6
BLG172	17 ^h 55 ^m 25 ^s .46	-31°19'20".6	BLG347	17 ^h 44 ^m 31 ^s .74	-24°20'58".8
BLG173	17 ^h 58 ^m 06 ^s .41	-31°19'21".3	BLG352	17 ^h 39 ^m 20 ^s .60	-21°09'30".0
BLG174	18 ^h 00 ^m 47 ^s .30	-31°19'21".6	BLG354	17 ^h 35 ^m 01 ^s .74	-23°39'32".1

general they assumed constant baseline and thus these methods cannot be applied to variable baseline events. Therefore, we applied the technique used previously for OGLE-I photometry (Udalski *et al.* 1994), which was an application of an earlier algorithm of Lupton *et al.* (1989). The method uses constant stars, separately in each field, to obtain correction factors to error bars for a given magnitude and the original error. Correction factors determined for I -band magnitudes from 15 to 18 range from 1.1 to 1.4, depending on the field. However, for bright measurements ($I \leq 15$ mag) corrections increase with increasing brightness, and can be as large as 2 to 3. Error bars of faint measurements (about 19–20 mag) were slightly over-estimated and had to be multiplied by 0.5–0.8.

All further analyzes were performed using rescaled photometry errors. Note that all magnitude measurements are only roughly calibrated, but as this only affects the zero-point of the light curve, it has little impact on our variability and microlensing studies.

5 Search Algorithm

We searched for microlensing events with variable baseline among all objects in the database for 82 selected OGLE-III Bulge fields. We analyzed each chip of each field separately; each chip contains from 60 to 270 thousand stars, depending on the stellar density.

First, from the error-corrected light curves we removed data points more than three standard deviations from the mean brightness of the whole light curve provided that their nearest neighboring points deviate by less than two standard deviations. Then, every object from the database exhibiting any kind of variation was investigated for the presence of a significant brightening peak. At this stage we applied the algorithm used in the search for microlensing events in the OGLE-II data as described in details in Sumi *et al.* (2006). The algorithm calculated the significance σ_i of each data point with respect to the baseline within a continuous running window, A, spanning half of the total time span of all measurements:

$$\sigma_i = \frac{I_{\text{med},B} - I_i}{\sqrt{\Delta I_i^2 + \sigma_B^2}} \quad (9)$$

where I_i and ΔI_i are the magnitude and error of the i th data point, respectively, and $I_{\text{med},B}$ and σ_B are, respectively, the median and standard deviation of the magnitude in window B, which is outside A. Fig. 4 schematically shows the idea of the search procedure. This procedure can detect events with both constant and small amplitude varying baselines, but in order to allow for larger amplitudes of variability we masked out all data points below the median of all magnitude measurements, as shown in Fig. 4.

In the next step for all the candidate light curves, we removed the brightening episode and checked the remaining data for periodicity in the range of 0.25 to 500 days. All the candidates were then inspected visually and as a result 21 events with periodic baselines were selected together with 111 candidates with

irregular baselines. In addition, we found five events with a few data points significantly below the constant baseline, which can potentially be caused by eclipsing variability. Tables 2 and 4 contain information for the periodic and irregular variables respectively. The name of each event is created with the same convention as used in previous OGLE catalogs (*e.g.*, Žebruň *et al.* 2001, Wyrzykowski *et al.* 2003) by joining the right ascension and declination, for example, the coordinates of OGLE180047.11–285934.5 are $\alpha_{2000} = 18^{\text{h}}00^{\text{m}}47\overset{\text{s}}{.}11$ and $\delta_{2000} = -28^{\circ}59'34\overset{\text{s}}{.}5$ (J2000). If an event was cross-identified with an object in the EWS, the latter designation is also given.

T a b l e 2
Microlensing event candidates with periodic baseline

name	period [d]	T_0 [HJD-245000]	I_0 [mag]	remarks (EWS)
OGLE174448.21-335605.4	0.36380	2123.73901	19.86 ± 0.18	2003-BLG-428
OGLE174841.52-352427.0	2.893016	2124.05151	18.17 ± 0.03	-
OGLE174913.88-334923.7	0.69884	2798.03955	19.69 ± 0.14	-
OGLE175239.94-322613.3	0.82756	2124.72705	19.02 ± 0.17	2002-BLG-103
OGLE175301.80-310449.9	0.533903	2790.37134	17.18 ± 0.02	-
OGLE175341.77-323002.2	0.644129	2125.40332	19.67 ± 0.20	-
OGLE175535.13-331533.3	7.13057	3512.74393	16.81 ± 0.01	-
OGLE175554.26-301826.7	4.026575	2112.56177	17.07 ± 0.01	2003-BLG-452
OGLE175646.40-304432.7	0.54399	2129.36426	17.83 ± 0.06	-
OGLE175708.46-302007.1	10.636035	2107.67065	16.71 ± 0.03	$P_2 = 1.10047$ d*
OGLE175828.21-304717.4	0.34825	2128.58350	18.00 ± 0.05	2004-BLG-390
OGLE175907.77-305519.1	0.86193	2147.69800	18.84 ± 0.09	2004-BLG-101
OGLE180047.11-285934.5	3.134806	2794.80420	15.52 ± 0.01	-
OGLE180502.14-293703.4	7.584951	2132.95898	19.98 ± 0.27	-
OGLE180503.30-293145.4	11.567380	2122.79810	17.59 ± 0.06	-
OGLE180834.52-255044.9	1.14626	3152.76758	19.75 ± 0.14	-
OGLE180950.21-260542.7	0.62610	2129.88306	18.93 ± 0.10	2002-BLG-093
OGLE181203.58-255823.5	0.539121	2129.54321	18.62 ± 0.06	-
OGLE181322.09-294846.4	53.2198	2107.63257	17.47 ± 0.03	2003-BLG-139
OGLE175618.55-294252.9	21.02317	2794.96635	14.174 ± 0.005	-
OGLE180540.47-273427.5	3.96628	2406.8730	17.21 ± 0.03	2004-BLG-081

*second, weaker period in the baseline

6 Events with Periodic Baselines

Light curves of events and their phase-folded periodic baselines are shown in Appendix A and listed in Table 2. The event baselines with periodic variability were modeled using Fourier harmonics. However, for three detached eclipsing vari-

Table 3

Best-fit microlensing model parameters for three events with periodic baseline

name	t_0 [HJD-2450000]	t_E [d]	u_0	f_s	χ^2	dof	model
OGLE174841.52-352427.0	2897.9 ±0.9	57.85 ±5.12	0.7461 ±0.0937	0.89 ±0.19	642.8	258	var.source
OGLE175907.77-305519.1	3095.0 ±0.1	21.37 ±2.59	0.1292 ±0.0211	0.35 ±0.04	449.0	280	var.blend
OGLE180047.11-285934.5	2847.1 ±0.1 2847.1 ±0.1	6.73 ±1.74 8.33 ±2.09	0.9567 ±0.3726 0.6731 ±0.2674	0.57 ±0.36 0.33 ±0.17	500.4 499.2	295 295	var.source var.blend

ables (OGLE174913.88–334923.7, OGLE175535.13–331533.3 and OGLE180047.11–285934.5) models were obtained with the EBAS code (Tamuz *et al.* 2006). Using a model of each event’s baseline we then fitted each event with a microlensing model as discussed in Section 2. In the majority of cases both the variable source and variable blend models did not converge to a unique model, mostly due to a small number of data points during the event of magnification. The model was only fitted to the data of three events. Table 3 presents the model parameters for each event, the value of the χ^2 and the number of degrees of freedom. The observed light curves of these three events are shown in Figs. 5–7 together with the models.

In the case of OGLE180047.11–285934.5 with eclipsing baseline (Fig. 7) both the variable source and variable blend models can fit the data with similar accuracy. We are unable to distinguish these two models mainly because the microlensing amplification for this event is very small, which causes the difference in the depths of amplified eclipses in these two models to be also small. The inset in Fig. 7 shows one data point, which occurred during the secondary eclipse almost at the peak of the event. However, this point is in agreement with both the variable source and variable blend models.

Another event with eclipsing baseline, OGLE175535.13–331533.3 was not fitted with the standard microlensing model with variable baseline, because its light curve exhibits both parallax and binary source effects. This event will be described and modeled in Wyrzykowski *et al.* (2006, in preparation).

The remaining events were not fitted with the variable baseline microlensing event model due to an insufficient number of data points collected during the events. The sparse sampling allows a variety of models to fit the data and the obtained parameters have large error bars.

Interestingly, in the baseline of the event OGLE175708.46–302007.1 we found another, weaker period. This object is probably a blend of two variables, of which the one with weaker and shorter period seems to be microlensed. However,

again we were not able to find a unique model to the data.

Two out of 21 events with periodic baseline, namely OGLE175618.55–294252.9 and OGLE180540.47–273427.5, shown in Fig. 8, are the most likely not caused by microlensing.

The light curve of the first one resembles binary microlensing event, which entered the caustic, however additional data collected in 2005 and at the beginning of 2006 (also presented in Fig. 8) show no signature of the second caustic crossing. Either it was missed in the gap between seasons, not happened yet or the event is not microlensing but caused by some other kind of variability, *e.g.*, a cataclysmic variable (CV) outburst. However, both hypotheses make this event unusual. Binary lens event would allow determination of the lens distance directly from the analysis of the baseline, assuming the observed variability comes from the lens. If this is a CV outburst the system would have very long period (21.02317 days) among CVs: the vast majority of CVs in the catalog of cataclysmic variables, CVCAT (Downes *et al.* 2001), have periods shorter than 5 days.

The shape of the second unusual event, OGLE180540.47-273427.5, cannot be explained with any known microlensing model. Its baseline folded with the period of 3.96628 days suggests a contact binary variable star and thus makes the CV outburst hypothesis plausible. However, again the period of variability is very long compared to known CVs and the shape of the brightening episode does not resemble that of CVs.

Both events require further analysis and additional follow-up photometric and spectroscopic observations to unveil their real nature.

7 Irregular Baseline Events

Table 4 lists 111 candidates for microlensing events with irregular variability in the baseline: their name, mean baseline brightness in *I*-band and cross-identification with events from the EWS, wherever possible. Appendix B presents the light curves of these events. All the light curves are shown for the time span of $2100 < \text{HJD} - 2450000 < 3350$ days. The minimum and maximum magnitudes of each event is shown in the upper (left and right, respectively) part of each panel.

There is a large variety of variability types in the baselines of presented events: from almost constant with some sporadic fluctuations to clear, large amplitude variability. The shape of most events with bright baselines ($\langle I \rangle \leq 16$ mag) resemble the OGLE Small Amplitude Red Giants (OSARGs, Wray, Eyer and Paczyński 2004), *e.g.*, OGLE174953.66–300640.8. The nature of the remaining variable baselines is not clear at the moment and requires further multicolor or spectroscopic observations.

Brightening episodes of the vast majority of the events resemble standard single lens microlensing, but there are also events which clearly exhibit exotic

Table 4

Microlensing event candidates with irregular baseline. At the bottom five possible eclipsing baseline events are listed.

name OGLE-	$\langle I_{\text{base}} \rangle$ [mag]	EWS	name OGLE-	$\langle I_{\text{base}} \rangle$ [mag]	EWS
173511.27-265652.5	16.22	2002-BLG-221	175559.20-284555.3	18.57	2002-BLG-076
173649.56-270326.5	17.07	-	175602.67-294724.3	13.52	-
173841.53-211137.1	15.04	2002-BLG-241	175603.52-335323.9	15.23	2003-BLG-311
173855.97-211617.9	19.49	-	175603.95-312649.7	16.21	-
174335.42-335711.5	17.63	2004-BLG-437	175623.74-304338.0	16.05	-
174346.78-342717.2	17.54	-	175624.81-323804.4	14.43	-
174422.49-334729.3	16.72	2003-BLG-212	175626.92-290430.1	15.03	-
174432.86-235842.4	15.74	-	175627.18-333626.0	15.30	-
174501.73-333707.2	13.95	-	175627.59-284211.8	16.21	2003-BLG-442
174522.43-333703.7	16.97	-	175631.70-304949.9	15.29	-
174635.41-334619.7	14.76	2004-BLG-361	175641.98-324243.6	14.28	2004-BLG-296
174635.42-334619.7	14.80	-	175657.24-330302.4	15.17	-
174635.76-332510.7	17.04	2003-BLG-010	175712.40-305041.4	16.39	-
174639.69-343542.6	14.08	-	175717.60-293513.2	13.90	2002-BLG-290
174657.43-331937.4	15.53	-	175743.18-285911.3	18.24	-
174732.74-340115.4	15.82	-	175746.93-295656.0	14.78	2004-BLG-077
174737.69-332338.1	16.62	2002-BLG-019	175747.82-300450.1	13.87	-
174825.61-232313.4	15.22	2003-BLG-430	175818.81-294918.7	15.18	-
174826.62-343333.0	14.57	-	175834.71-295834.3	15.88	2004-BLG-026
174904.99-345252.3	13.12	-	175846.00-290743.3	15.47	2004-BLG-029
174921.09-352558.8	14.60	-	175903.04-271119.8	15.57	2003-BLG-095
174938.25-223143.1	14.74	-	175912.23-295324.2	17.08	-
174951.98-303628.8	15.42	-	175919.19-295316.1	14.64	2004-BLG-580
174953.66-300640.8	16.08	2004-BLG-009	175941.94-283506.7	15.62	-
174954.62-351932.1	15.20	-	180024.58-313821.2	15.56	-
175020.91-342856.1	15.88	-	180029.65-291209.7	17.63	2002-BLG-356
175047.59-293005.0	16.34	2003-BLG-120	180032.79-315100.3	17.63	2003-BLG-389
175111.06-294754.1	14.21	-	180035.39-322702.6	15.43	2003-BLG-088
175120.74-302655.6	14.02	-	180051.26-311244.1	15.62	2003-BLG-035
175121.12-294109.3	18.28	-	180112.43-294812.0	13.42	-
175125.38-322147.6	15.77	-	180129.50-302841.5	18.00	-
175130.07-290810.3	15.85	-	180149.88-312136.2	18.66	2003-BLG-034
175134.32-295519.3	16.76	2002-BLG-193	180209.11-301101.4	15.64	2003-BLG-135
175206.25-292116.6	15.19	-	180215.81-320242.2	18.10	2004-BLG-145
175221.14-333426.9	13.89	-	180308.17-314411.6	16.04	2002-BLG-034
175226.40-292432.0	14.35	-	180314.20-273106.6	15.33	-
175235.04-334343.1	15.86	-	180348.19-293301.8	15.69	-
175239.24-290150.1	16.69	2004-BLG-362	180359.54-314950.2	14.28	-
175256.12-294509.2	17.59	-	180423.57-285120.0	13.29	-

Table 4

Concluded

name OGLE-	$\langle I_{\text{base}} \rangle$ [mag]	EWS	name OGLE-	$\langle I_{\text{base}} \rangle$ [mag]	EWS
175257.97-300626.3	18.11	-	180424.07-315220.7	16.95	2002-BLG-137
175308.43-304353.9	14.61	-	180424.59-275340.7	16.47	-
175341.55-303119.0	16.65	-	180429.93-290550.3	17.61	-
175350.55-293117.7	14.18	-	180507.09-274309.2	16.63	-
175355.20-291021.5	17.42	2002-BLG-041	180542.81-323020.2	18.20	-
175405.62-314555.2	16.25	2004-BLG-018	180613.39-283613.4	18.58	-
175409.89-285636.9	17.36	-	180623.05-303612.4	18.71	-
175417.90-295058.1	14.27	-	180625.20-310346.4	16.39	2003-BLG-171
175422.81-302324.5	14.98	2004-BLG-600	180628.66-273742.9	13.38	2004-BLG-383
175425.39-355519.5	15.12	-	180638.79-274702.3	13.13	-
175435.35-291929.0	15.93	-	180700.89-274548.4	15.93	-
175440.01-315035.3	16.32	-	180903.23-255755.1	15.12	-
175453.32-304307.4	15.07	-	180926.89-270716.2	14.87	2003-BLG-133
175455.98-290113.8	16.57	-	180933.92-292018.8	15.26	-
175456.39-295441.5	13.95	2004-BLG-290	181054.57-272434.9	16.48	2004-BLG-051
175459.82-335325.9	18.23	-	181332.21-281254.9	15.43	-
175500.72-310411.0	18.76	-			
173551.54-271144.9	14.67	2002-BLG-220	175606.17-293334.4	13.99	-
175206.95-340704.2	16.18	-	175933.80-300000.6	15.74	-
175320.16-293003.7	16.17	2002-BLG-363			

behavior, *e.g.*, OGLE175912.23–295324.2 or OGLE180209.11–301101.4, caused probably by a binary lensing system (*e.g.*, Mao and Paczyński 1991).

In the analyzed dataset, in addition to 21 with periodic and 111 with irregular baselines, we found 5 events with several data points significantly below their mean baseline brightness. These events are listed at the bottom of Table 4 and their light curves are shown in the last five panels in Appendix B. Some of the outlying data points are likely caused by instrumental effects or bad weather, however some can be signatures of eclipses. As their number is usually two or three it is impossible to determine any periodicity. In order to detect and confirm eclipses more observations or dedicated follow-up is necessary. Events with eclipsing variability in the baseline are one of the most valuable, as their baselines can be used for determining information about the lens and the source. Two of these events are particularly suspected to be in fact binary source microlensing events: OGLE173551.54–271144.9 and OGLE175206.95–340704.2, as their light curves exhibit some small systematic deviations from the standard model during the magnification. Such events may in some cases lead to a unique

determination of the lens mass (Wyrzykowski *et al.* 2006, in preparation).

8 Variable Events Warning System

Most of the events presented in this paper with periodic baselines were not fitted with any model due to the small number of observations taken during the magnification. These cases are unfortunately lost. However, in order to make good use of forthcoming events it is necessary to detect them in the early stage of microlensing and then follow them up, especially during the highest magnification.

Here we briefly describe a system, called Variable Events Warning System (VEWS), a preliminary version of which is already working as an extension of the existing OGLE Early Warning System (EWS). Similar to the EWS (Udalski 2003), the new system checks the incoming photometric data from the telescope in order to detect possible microlensing brightenings. These two systems are complementary as the EWS investigates only constant stars, while the VEWS checks variable stars. As mentioned above, the most valuable variable baseline events are those with eclipsing baseline variability, as they can be used to determine the lens or source distances directly, as well as other parameters of the event. As a first attempt, VEWS is based only on the catalog of eclipsing variables. Currently the VEWS uses about 7000 stars, selected from the catalog of about 10000 eclipsing binaries found by Devor (2005) in the OGLE-II Galactic bulge data, which were cross-correlated with stars in 56 OGLE-III Bulge fields frequently monitored since 2006. In the future the VEWS will be based on a complete set of eclipsing variable stars in the OGLE-III Galactic bulge data, when such a catalog becomes available.

As a result the system produces alerts of possible ongoing microlensing events of eclipsing variable stars. Detailed information of any event and the baseline eclipsing binary star will be provided to observers worldwide and shown at the OGLE EWS website[‡] to allow photometric and spectroscopic follow-up observations by other observatories.

The detection rate of events with periodic baselines is expected to be around seven per year, with at least three on eclipsing variable stars. This estimate is based on our detection of 13 new periodic baseline events, not detected by the EWS (6 new eclipsing) in comparison with 1137 events detected by the EWS in our 82 fields in years 2001–2004. Assuming a typical OGLE detection rate of 600 regular microlensing events per year, we expect half a dozen microlensing events with periodic variable baselines per season.

9 Conclusions

In this paper we presented microlensing events with variable baselines and showed that they are common in the Galactic bulge fields. Analysis of vari-

[‡]<http://ogle.astroww.edu.pl/ogle3/ews/ews.html>

ability amplitude behavior during gravitational microlensing amplification may lead to the determination of parameters of the event, removing common degeneracy due to blending. The change of the variability amplitude depends on the blending parameter f_s , whose determination is an important issue in almost all microlensing problems. For example, in the optical depth determinations, an incorrect blending parameter may dramatically change the timescale of an event and thus affect the estimated optical depth (e.g., Sumi *et al.* 2006).

In addition, events with variable baseline can also potentially be used for the determination of physical parameters of the microlensing event, which are not measurable for a standard microlensing event. Using characteristics of a given variability type, *e.g.*, eclipsing binary, Cepheid or RR Lyrae, it might be possible to obtain the distance to the source, if the variable star acts as the lensed source. Another interesting possibility may occur if the lensing object is a variable and acts as a blend. In such cases, especially when there are binary lens signatures in the light curve and eclipsing variability in its baseline, it might be possible to determine the distance and even the mass of the lens, which was so far only possible for very few events (*e.g.*, Alcock *et al.* 2001, An *et al.* 2002, Jiang *et al.* 2004).

In order to allow detailed follow-up observations of interesting variable baseline events we are testing the Variable Events Warning System (VEWS), which can detect microlensing brightening occurring on eclipsing binary stars.

Acknowledgements. We would like to thank Profs. Bohdan Paczyński, Tsevi Mazeh and Drs. Vasily Belokurov, Wyn Evans, Martin Smith, Omer Tamuz and Szymon Kozłowski for their continuous support for this project.

This paper was partially supported by the MNiSW BST grant to the Warsaw University Observatory, NSF grant AST-0204908, NASA grant NAG5-12212 and by the European Community's Sixth Framework Marie Curie Research Training Network Programme, Contract No. MRTN-CT-2004-505183 "ANGLES". LW also acknowledges support from the visitor programme at the Jodrell Bank Observatory.

REFERENCES

Alard, C., and Lupton, R. 1998, *Astrophys. J.*, **503**, 325.
 Alcock, C., *et al.* 1993, *Nature*, **365**, 621.
 Alcock, C., *et al.* 2001, *Nature*, **414**, 617.
 An, J.H., *et al.* 2002, *Astrophys. J.*, **572**, 521.
 Assef, R.J., *et al.* 2006, *Astrophys. J.*, , accepted, astro-ph/0604147.
 Collinge, M. 2004, , astro-ph/0402385.
 Devor, J. 2005, *Astrophys. J.*, **628**, 411.
 Downes, R.A., Webbink, R.F., Shara, M.M., Ritter, H., Kolb, U., and Duerbeck, H.W. 2001, *P.A.S.P.*, **113**, 764.
 Jiang, G., *et al.* 2004, *Astrophys. J.*, **617**, 1307.
 Lupton, R.H., Fall, S.M., Freeman, K.C., and Elson, R.A.W. 1989, *Astrophys. J.*, **370**, 201.
 Mao, S., and Paczyński, B. 1991, *Astrophys. J. Letters*, **374**, L37.
 Mizerski, T., and Bejger, M. 2002, *Acta Astron.*, **52**, 61.
 Paczyński, B. 1986, *Astrophys. J.*, **304**, 1.

Snodgrass, C., Horne, K., and Tsapras, Y. 2004, *MNRAS*, **351**, 967.

Sumi, T., Woźniak, P.R., Udalski, A., Szymański, M., Kubiak, M., Pietrzyński, G., Soszyński, I., Żebruń, K., Szewczyk, O., Wyrzykowski, Ł., and Paczyński, B. 2006, *Astrophys. J.*, **636**, 240.

Szymański, M., and Udalski, A. 1993, *Acta Astron.*, **43**, 91.

Tamuz, O., Mazeh, T., and North, P. 2006, *MNRAS*, **367**, 1521.

Udalski, A. 2003, *Acta Astron.*, **53**, 291.

Udalski, A., Szymański, M., Kałużny, J., Kubiak, M., Krzeminski, W., Mateo, M., Preston, G. W., and Paczyski, B. 1993, *Acta Astron.*, **43**, 289.

Udalski, A., Szymański, M., Stanek, K. Z., Kałużny, J., Kubiak, M., Mateo, M., Krzeminski, W., Paczyński, B., and Venkat, R. 1994, *Acta Astron.*, **44**, 165.

Udalski, A., Kubiak, M., and Szymański, M. 1997a, *Acta Astron.*, **47**, 319.

Udalski, A., Szymański, M., Kubiak, M., Pietrzyński, G., Woźniak, P., and Żebruń, K. 1997b, *Acta Astron.*, **47**, 431.

Woźniak, P.R. 2000, *Acta Astron.*, **50**, 421.

Wray, J.J., Eyer, L., and Paczyński, B. 2004, *MNRAS*, **349**, 1059.

Wyrzykowski, Ł., Udalski, A., Kubiak, M., and Szymański, M., Żebruń, K., Soszyński, I., Woźniak, P.R., Pietrzyński, G., and Szewczyk, O. 2003, *Acta Astron.*, **53**, 1.

Żebruń, K., Soszyński, I., Woźniak, P.R., Udalski, A., Kubiak, M., Szymański, M., Pietrzyński, G., Szewczyk, O., and Wyrzykowski, Ł. 2001, *Acta Astron.*, **51**, 317.

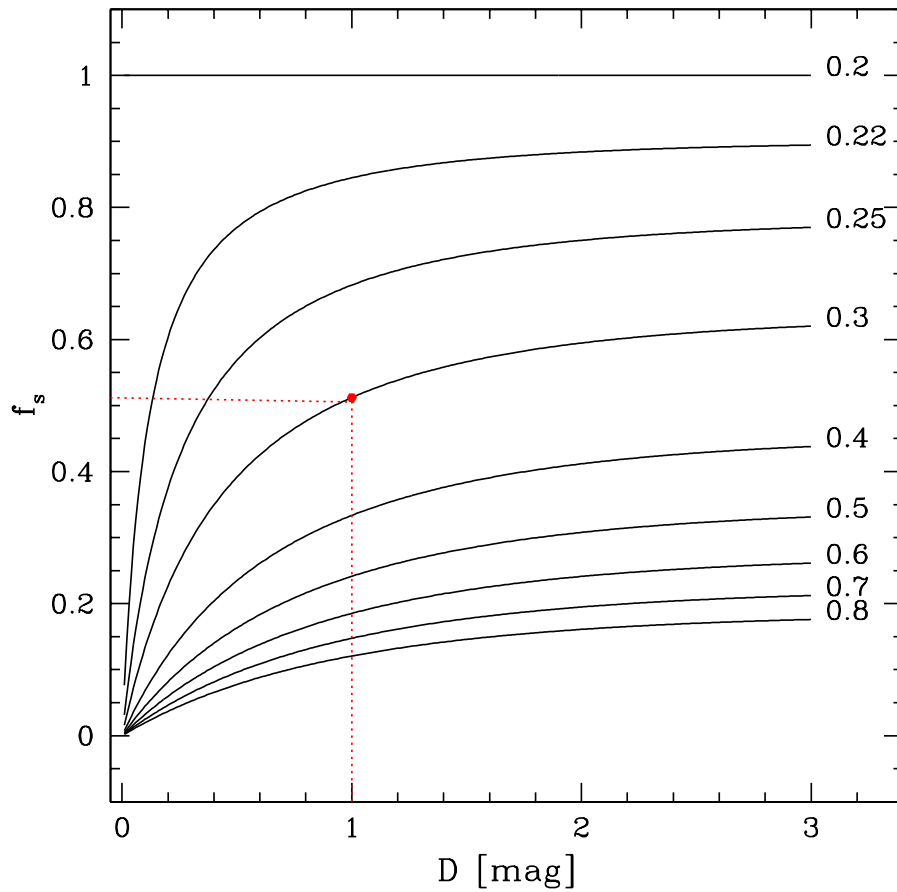


Fig. 3. Example plot for determining the blending parameter from the microlensing light curve of a variable source event with baseline amplitude 0.2 mag. The dashed lines show how to determine f_s if the amplified amplitude equals $\Delta I_A = 0.3$ mag on top of the brightening of $D_{\text{mag}} = 1$ mag. $f_s = 0.51$ for this example.

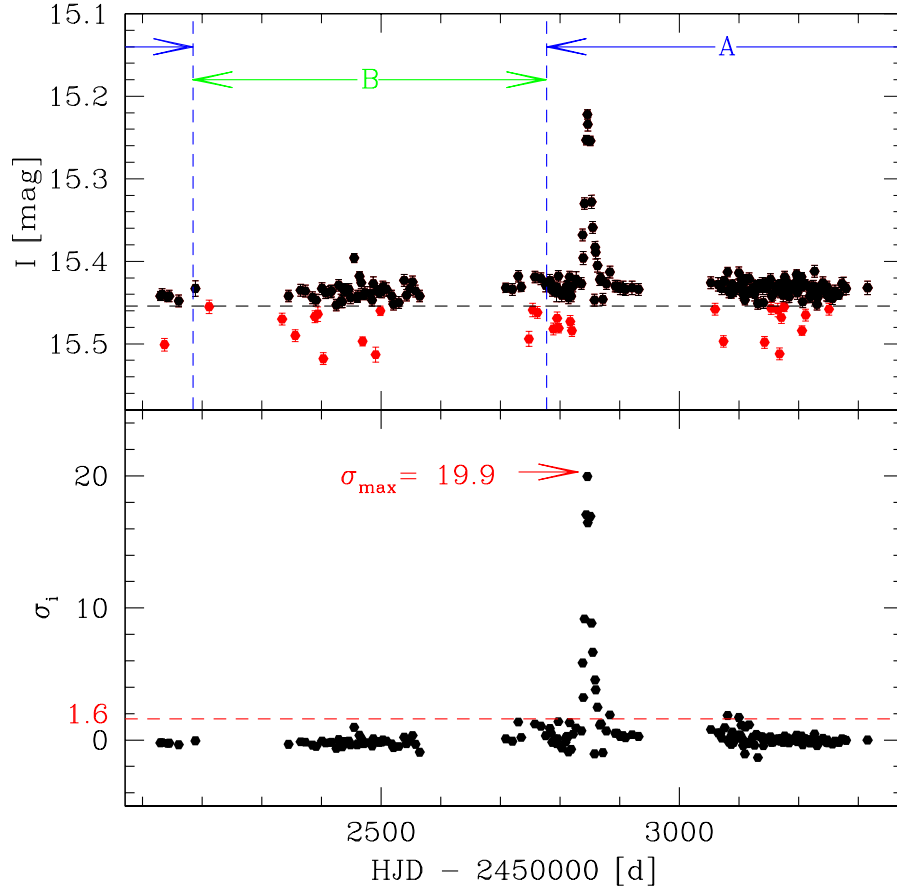


Fig. 4. Visualization of the search procedure. The upper panel shows the light curve of an event with eclipsing variability in the baseline. Points below the median (horizontal dashed line) were excluded from significance calculations. The significance of the central point of the window A was calculated with respect to the data in window B. The lower panel shows the significance calculated for each data point. The minimum detection threshold of 1.6 and the maximum significance value for this event are marked.

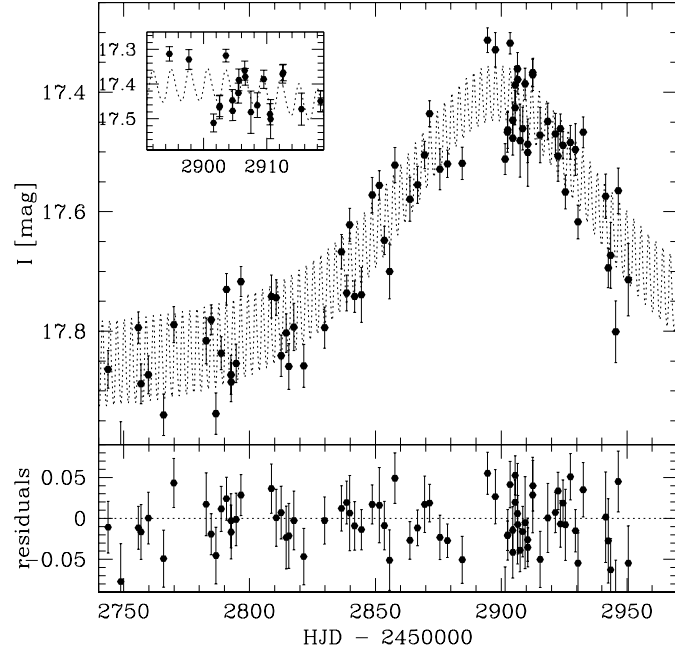


Fig. 5. Data and best-fit microlensing models with variable baseline of event OGLE174841.52–352427.0. The dotted line shows the variable source model.

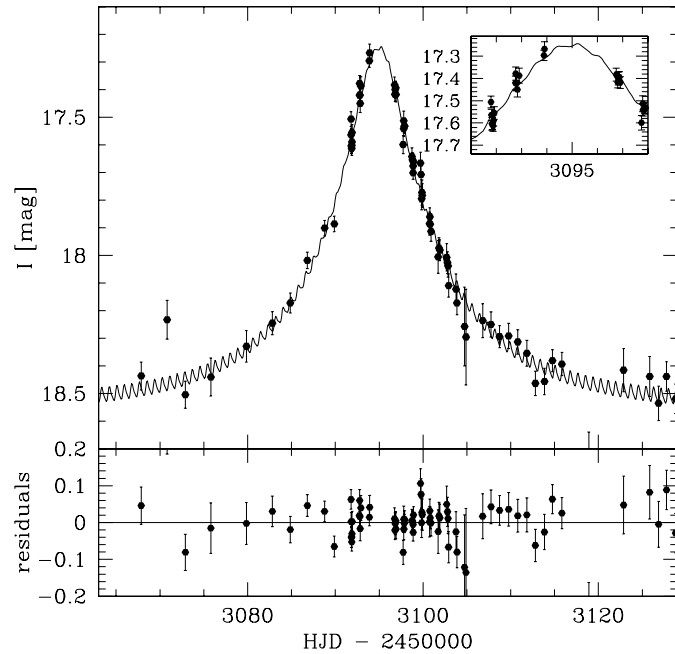


Fig. 6. Data and best-fit microlensing models with variable baseline of event OGLE175907.77–305519.1. The solid line shows the variable blend model.

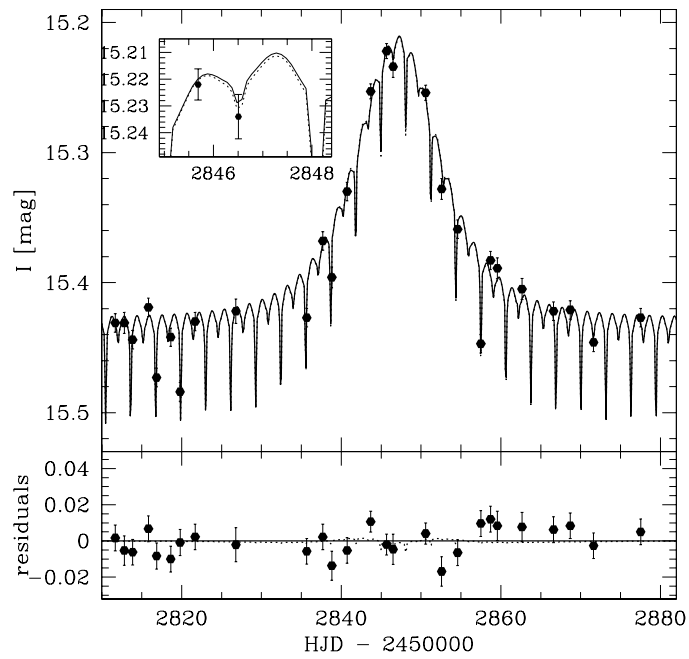


Fig. 7. Data and best-fit microlensing models with variable baseline of event OGLE180047.11–285934.5. The dotted and solid lines are for the variable source and variable blend models, respectively.

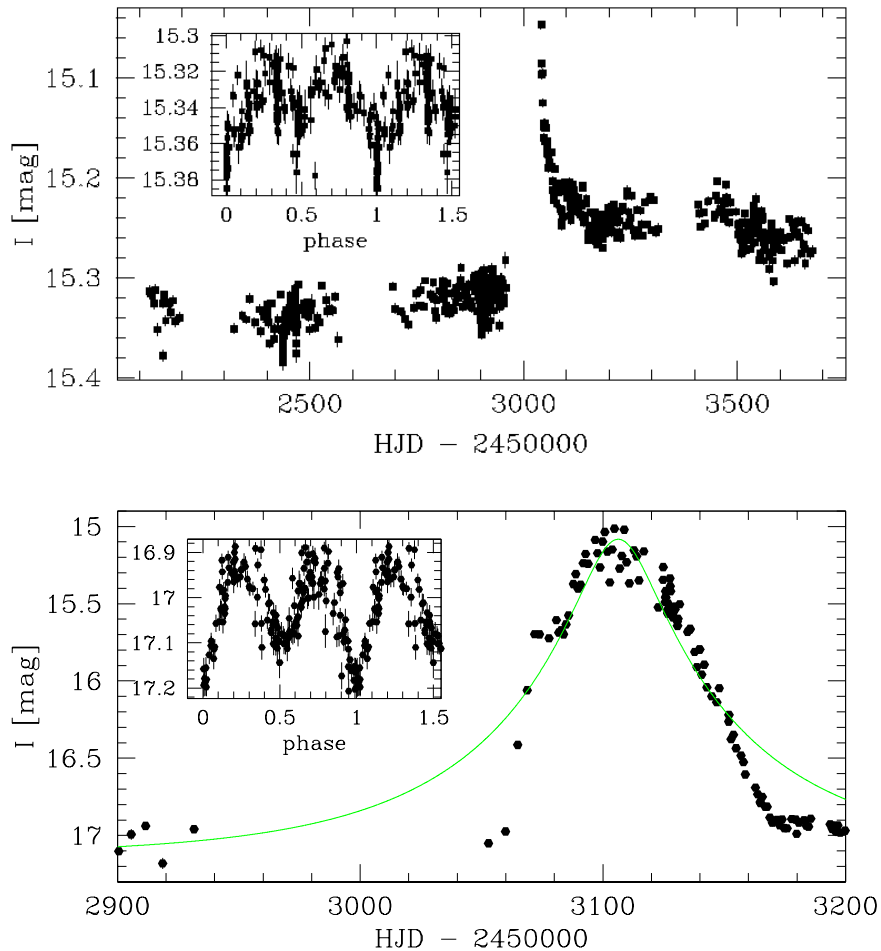
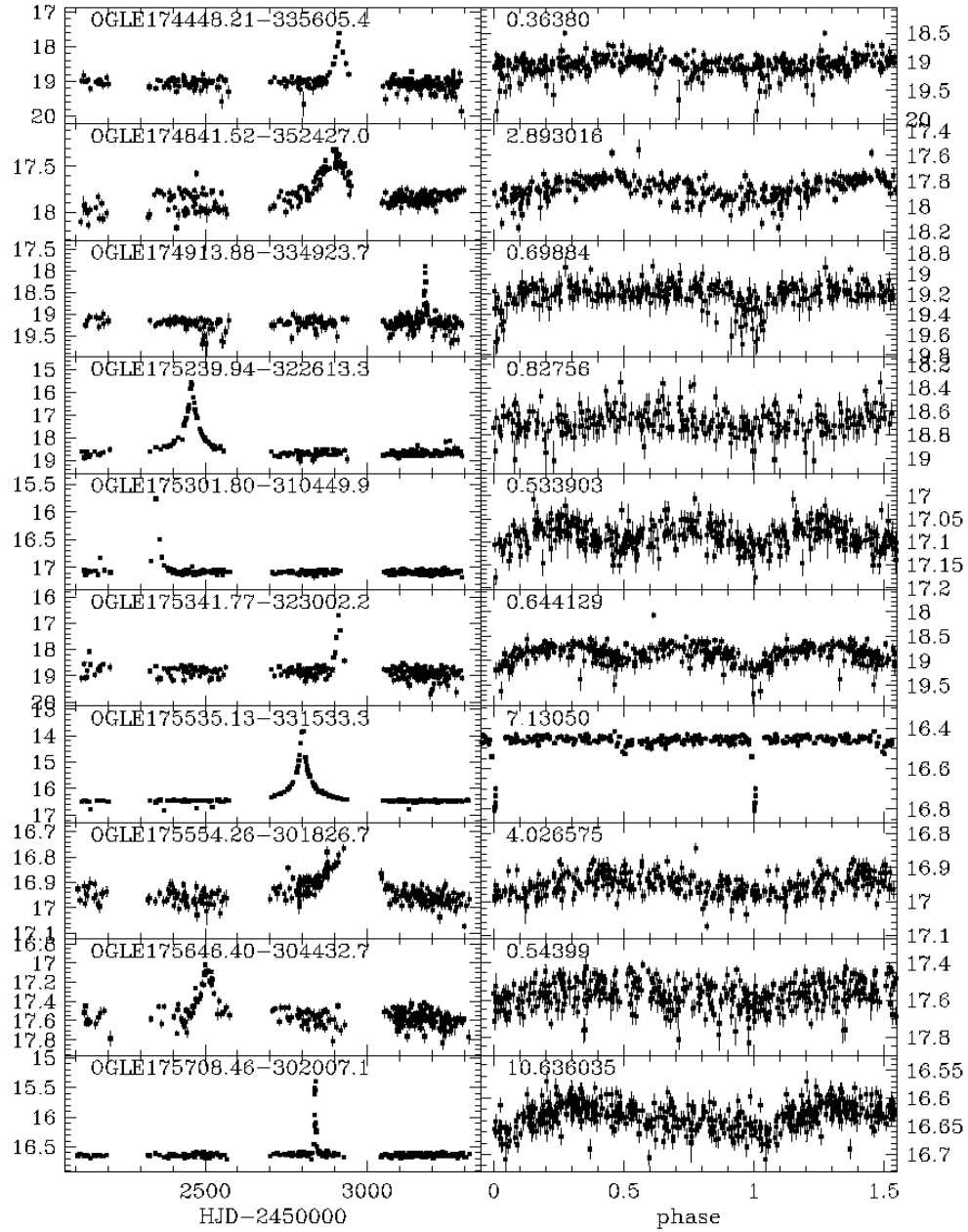


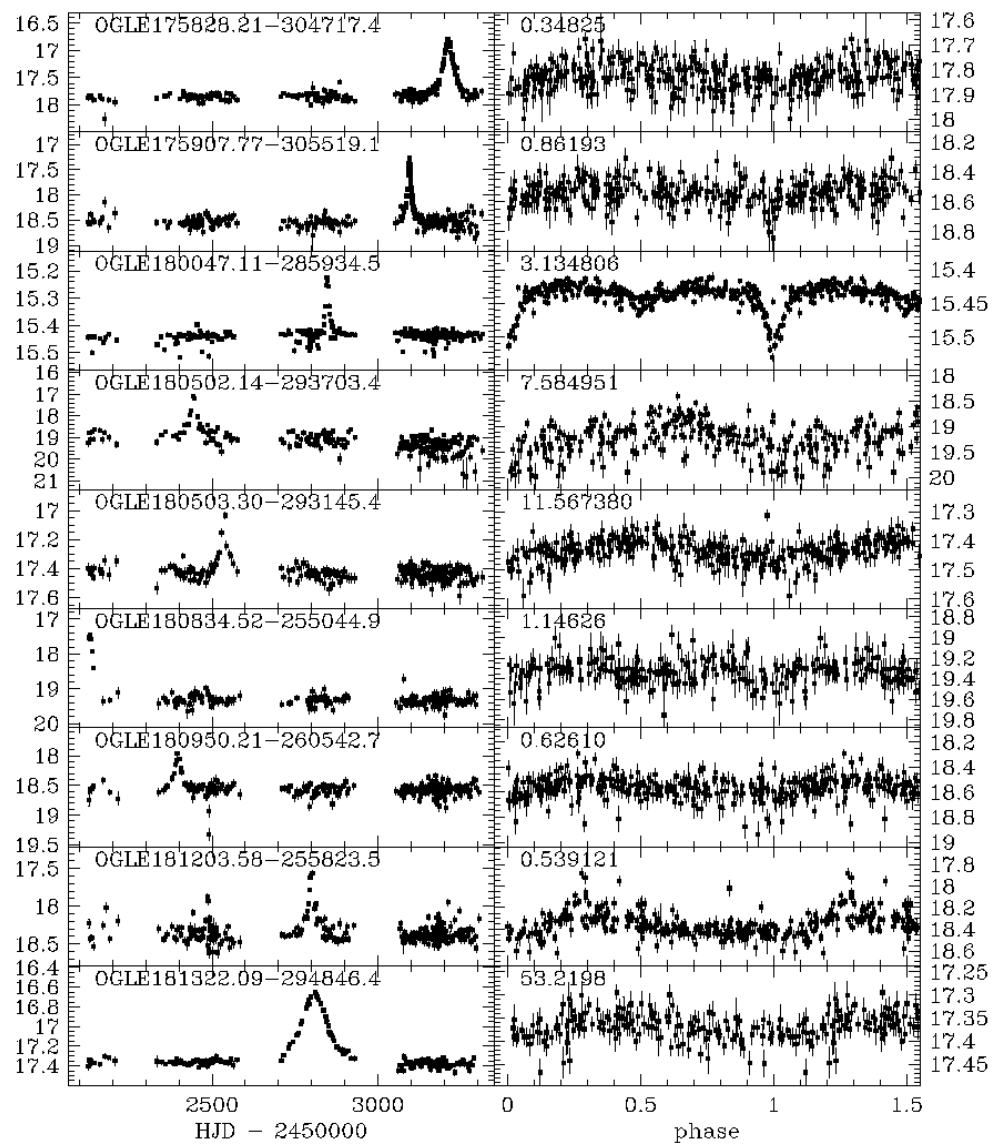
Fig. 8. Light curves of OGLE175618.55-294252.9 (top) and OGLE180540.47-273427.5 (bottom, with the best-fit standard model). The insets show their baselines phase-folded with a period of 21.02317 and 3.96628 days, respectively. The first event may be a binary lensing event, where the second caustic crossing was missed or has not happened yet, or it is an eruptive variable star. The nature of the second event is unclear.

Appendix A

Microlensing events candidates with periodic variability in the baseline

The left column contains the whole light curve of the event and its name while the right column shows the phase-folded baseline and period in days.





Appendix B

Candidates for microlensing events with irregular variability in the baseline

The horizontal scale is the HJD-2450000 spanning from 2100 to 3350 days.

The numbers in each panel are the minimum (*left*) and maximum (*right*) brightness in magnitudes in the *I*-band. The last five events are potential eclipsing baseline events listed at the end of Table 4.

